Proceedings of 20th International Congress on Acoustics, ICA 2010

23-27 August 2010, Sydney, Australia

# Influence of defective elements on acoustic field and imaging for a linear array transducer

**Kwang-Yoon Choi (1), Kang-Lyeol Ha (1), Moo-Joon Kim (1), Jung-Soon Kim (2) and Chae-Bong Lee (3)**

(1) Pukyong National University, 599-1 Daeyeon 3-Dong, Nam-Gu, Busan, Korea, (2) Tongmyong University, 179 Sinseonno, Nam-Gu, Busan, Korea (3) Dongseo University, San 69-1 Jurye Dong, Sasang-Gu, Busan, Korea

**PACS:** 43.38.Hz, 43.80.Qf

## ABSTRACT

The transient ultrasonic fields and the B-mode images of a linear array medical transducer which has a few defective elements were obtained by simulation and the results were compared with those of a normal transducer. The center frequency of the transducer was 7.5 MHz and the acoustic beam was formed by 64 active elements including the defective ones among the total number of 192. It was shown that the fields by the transducer with defective elements spread widely on the lateral direction due to enhancement of sidelobe level. The spurious images beside that of a point target were appeared and the lateral spatial resolution was degraded significantly with increment of the number of defective elements.

## INTRODUCTION

Ultrasonic transducer is one of the most important components in a medical diagnostic imaging system. Generally, the transducer has many piezoelectric elements which are arrayed in one or two dimensions. The beamforming using a part of the elements, called as active elements, is carried out to make a confined acoustic beam and the beam is electronically scanned with radiating acoustic pulses into the medium of human body sequentially in a linear array transducer. For reduction of sidelobe level, the apodization which is amplitude weighting of exciting electric signals is taken in the beamforming[1]. The images are obtained by signal processing of the envelopes of reflected waves from the boundaries with different acoustic impedance in the medium. The waveform of the radiated pulse at a point in the medium is constructed by the superposition of wavelets from every active element according to the Huygens' Principle. If some of the active elements do not work due to defects such as crack, cable disconnection and so on, not only the waveform but the acoustic field will be changed. Consequently, it affects on the acoustic imaging, so that the obtained image is changed. However, the defective transducers have been using in practical diagnosis and it is known that the discrimination between the images by a defective probe and by a normal one is not easy to recognize if only a few elements are faulty. Recently, the effect of transducer defect on image quality and the method of defective transducer evaluation have been studied by several researchers[2-5]. In this study, the influence of a few defective elements on transient acoustic fields and on imaging for a linear array transducer with 192 piezoelectric elements was analyzed by simulation. The center frequency of the transducer is 7.5 MHz and the number of active elements for beamforming is 64. The apodization with Hanning window was mainly taken in the beamforming. The variation of the lateral and the axial resolution according to the number of defective elements was discussed.

## STRUCTURE AND OPERATING CONDITIONS OF THE TRANSDUCER

The schematic structure of the transducer examined in this study is shown in Figure 1. It has linearly arrayed 192 piezoelectric elements with inter-element spacing $D = 0.125$ mm. As shown in Table 1, the elevation length $L = 4.0$ mm and the width $W = 0.2$ mm for the individual element of which center frequency is 7.5MHz. The mechanically fixed focus by

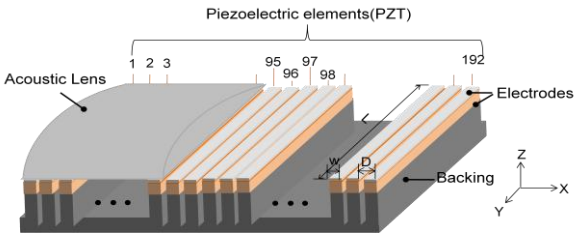


Figure 1. Schematic structure of the linear array transducer.

Table 1. Dimension and operating conditions of the linear array transducer.

| | |
|---|---|
| Number of total elements | 192 |
| Number of active elements | 64 |
| Element width [mm] | 0.1 |
| Elevation length [mm] | 4.0 |
| Kerf [mm] | 0.025 |
| Center frequency [MHz] | 7.5 |
| Mechanical focal distance [mm] | 20.0 |
| Dynamic transmit focus [mm] | 10, 20, 30, 40 |
| Apodization | Hanning |
| Speed of sound in medium [m/s] | 1540 |

the curvature of acoustic lens is 20.0 mm. It is assumed that every element has same characteristics and the beamforming is performed by 64 elements with Hanning apodization for sidelobe reduction. The dynamic transmit foci are set at 10, 20, 30, 40 mm from the radiation surface of the transducer. Five cases of defect that one element of #96(N=1), two elements of #96 and #97(N=2), three elements of #95~#97(N=3), four elements of #95~#98(N=4) and five elements of #94~#98(N=4) are faulty, were considered, respectively. The middle of the elements of #96 and #97 is the lateral center of the transducer. If the beam is formed by the elements of #65~#128, the defective elements are positioned near the center of the active elements. For comparison, the characteristics of normal transducer(N=0), which does not have any defective element, was also analyzed. In the calculation, each element is devided by $8 \times 156$ with assuming as a set of simple point sources with $\lambda/8$ interval on a semi-infinite baffle.

## SIMULATION RESULTS

### Ultrasonic Fields

The ultrasonic fields for many types of normal transducer are readily simulated by the Field-II program[6-8]. In this study, we modified the program for the array transducer with some defective elements. The simulated results showed that the acoustic field by the transducer is changed dramatically with the number of the defective elements. As an example, the contour graphs of the normalized transient fields near $z = 20$ mm from the radiation surface are shown in Figure 2. In the

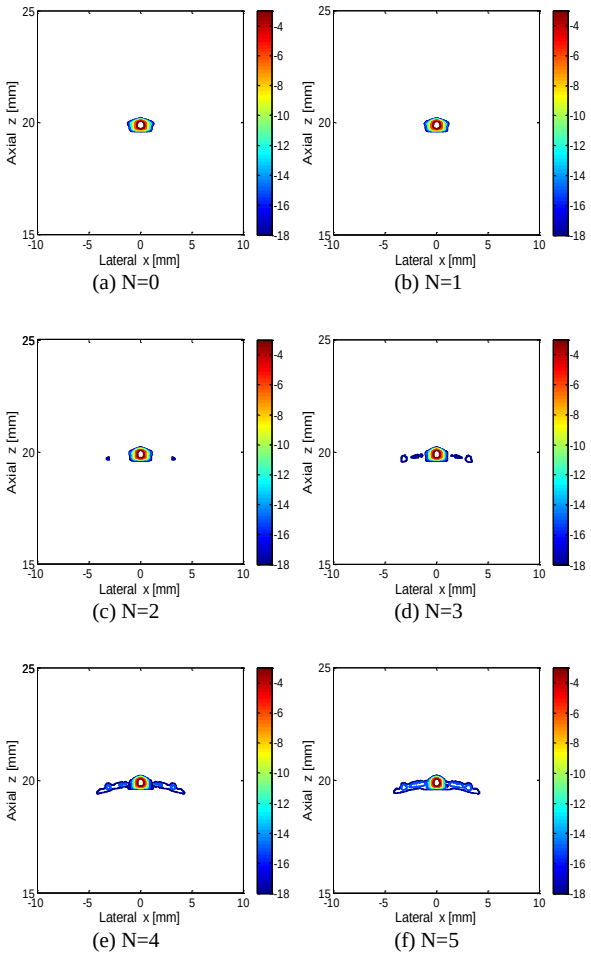


(a) N=0 (b) N=1

(c) N=2 (d) N=3

(e) N=4 (f) N=5

Figure 2. Transient acoustic fields near $z = 20$ m from the radiation surface.

calculation, the attenuation and multi-reflection in the acoustic lens is ignored, and the initial particle velocities on the surface of defective elements were considered as zero. The exciting pulse is assumed as a two-cycle RF pulse with Hanning envelope. Every figure includes six contour lines of -3, -6, -9, -12, -15 and -18 dB. It is noted that fields by the transducer with defective elements spread widely on lateral(azimuth) direction. For detail analysis, the pressure level distributions on the lateral axis including the maximum amplitude near $z = 20$ mm are shown in Figure 3. As shown in the figure, the SPL on the acoustic axis(x=0), that is the center of mainlobe, decreases gradually while the number of defective elements increase. The difference of peak values between N=0 and N=5 is about -1.5 dB. On the other hand, the SPL outside of the mainlobe increases rapidly. The local maximum of the 2nd sidelobe is appeared near $\pm 1.7$ mm on the lateral axis when it is operated by continuous wave. For N=5, the increment of SPL from the normal transducer is about 14.7 dB at that region. The similar tendency of SPL variations was shown for the targets at different axial distance. In the pressure level distributions on the axial axis($x = 0$), however, the difference according to the number of defective elements was very small as shown in Figure 4.

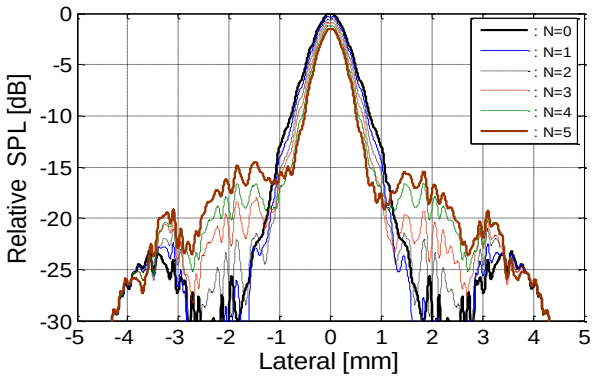


Figure 3. Acoustic pressure distribution on the lateral axis including the maximum amplitude near $z = 20$ mm.

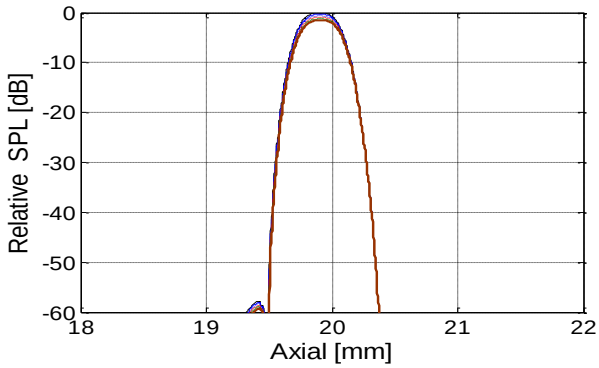


Figure 4. Acoustic pressure distribution on the axial axis with $x = 0$.

### Influence on B-mode Imaging

The simulated B-mode images for four point targets in homogeneous medium of which sound velocity is 1540 m/s are shown in Figure 5. Each image frame consists of 40 image lines and the #44~#148 elements were used so as to make an image frame. The targets locate at 10~40 mm with separation of 10 mm from the radiation surface. The dynamic range of the system for imaging was set by 60 dB. According to the number of defective elements, the images for every target are broadening along the lateral direction so that the lateral resolution decreases. The change in the axial direction is so small that it is difficult to catch up any difference with the naked

eye. Using the pixel values for the proper line in an image displayed on a monitor, the lateral or the axial resolution R can be obtained by following equation[8].

$$R = \frac{FWHM}{\sqrt{\ln 2}} \sqrt{\ln\left(\frac{A}{A-JND}\right)} - D, \quad (1)$$

where, FWHM is the full width half maximum, A is the maximum, JND is the just noticeable difference, and D is the diameter of a target. The profiles of the pixel value along the acoustic axis(x=0) and the lateral axis at z=20 mm are shown in Figure 5. The profiles show the similar pattern with SPL distributions. The Gaussian PSF(Point Spreading Function) for every main-lobe was estimated by numeric fitting, and then the parameters of the eq.(1) were obtained from the PSF. Table 2 shows the spatial resolutions which were obtained using the pixel values of the lateral and the axial lines for the image at $z = 20$ mm and at $x = 0$, respectively. It is shown that the lateral resolution varies significantly with the number of defective elements, although the variation of axial resolution is negligible. The tendency of spatial resolution variation was also shown for the other targets, and it is well agree with the experimental results reported by Yang et al.[5].

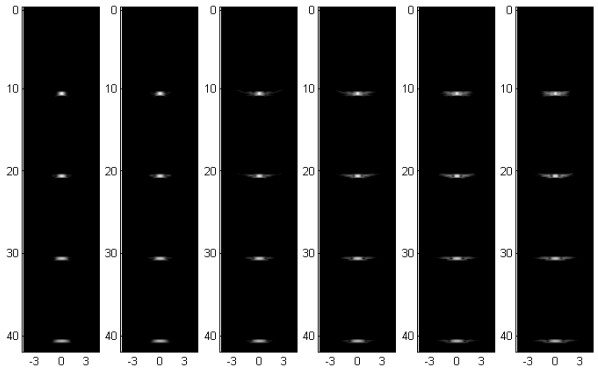

(a) N=0 (b) N=1 (c) N=2 (d) N=3 (e) N=4 (f) N=5

Figure 5. B-mode images for four point targets.

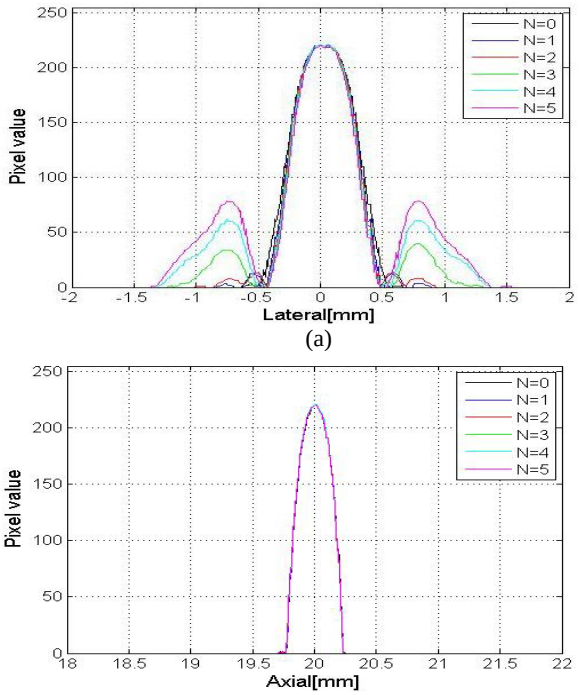


Figure 6. Pixel value profiles along the lateral axis at z=20 mm (a) and the acoustic axis x=0 (b).

Table 2. Variation of spatial resolutions obtained by the pixel value profiles at z=20mm.

| Numbers of faulty elements | Axial resolution (mm) | Lateral resolution (mm) |
|---|---|---|
| 0 | 0.238 | 0.926 |
| 1 | 0.238 | 0.901 |
| 2 | 0.237 | 0.871 |
| 3 | 0.236 | 0.848 |
| 4 | 0.236 | 0.830 |
| 5 | 0.236 | 0.815 |

## CONCLUSION

In this study, for a linear array transducer with a few defective elements, the transient ultrasonic fields and the B-mode images were simulated using the modified Field-II program, and the results were compared with those of a normal transducer. The center frequency of the transducer is 7.5 MHz and the acoustic beam is formed by 64 active elements including the defective ones among the total number of 192. It is shown that the fields by the transducer with defective elements spread widely on the lateral direction due to the enhancement of sidelobe level. The spurious images beside that of a point target were appeared. The lateral spatial resolution was degraded significantly with increment of the number of defective elements, although the variation of axial resolution is negligible.

## REFERENCES

1 G.S. Kino, *Acoustic waves: devices, imaging, and analog signal processing*, Prentice-Hall, Inc., Englewood Cliffs, pp. 387-391 (1987)

2 B. Weigang, G.W. Moore, J. Gessert, W. H. Phillips and M. Schafer, "The methods and effects of transducer degradation on image quality and the clinical efficacy of diagnostic sonography," *Jour. Diag. Med. Sonography*, vol. 19, no. 1, pp. 3-13 (2003)

3 B.C. Yoo, H.H. Choi, S.C. Noh, H.K. Min and J.W. Kwon, "A study of testing method for diagnostic ultrasonic array probe through pattern analysis of acoustic-fields with probe channel division" *J. Biomed. Eng. Res*, **27**, pp. 229-236 (2006)

4 M. Martensson, M. Olsson, B. Segall, A. G. Fraser, R. Winter and L. Brodin, "High incidence of defective ultrasound transducers in use in routine clinical practice," *Euro. Jour. Echocardiography*, **10**, pp. 389-394 (2008)

5 J.H. Yang, K.S. Lee, G.S. Kang, D.G. Paeng and M.J. Choi, "Effects of ultrasonic probe defects on the spatial resolution of B-mode images" *Proceedings of the ASK-Symposium*, **28(1S)**, pp. 176-179 (2009)

6 http://server.electro.dtu.dk /personal/jaj/field/, (2009)

7 J.A. Jensen, " Field: A program for simulating ultrasound systems", *Medical & Biological Engineering & Computing*, **34**, Supplement 1, Part 1, pp. 351-353 (1996)

8 J.A. Jensen and N. B. Svendsen, "Calculation of pressure fields from arbitrarily shaped, apodized, and excited ultrasound transducers" *IEEE Trans. Ultrason., Ferroelec., Freq. Contr.*, **39**, pp. 262-267 (1992)